Journal of Materials Chemistry

Cite this: *J. Mater. Chem.*, 2011, **21**, 15121

www.rsc.org/materials

FEATURE ARTICLE

Medical applications of inorganic fullerene-like nanoparticles

A. R. Adini,[ab] M. Redlich[b] and R. Tenne[a]

Received 24th April 2011, Accepted 7th June 2011
DOI: 10.1039/c1jm11799h

Nanoparticles of layered compounds, like MoS_2 and WS_2, having hollow closed-cage structures and known as fullerene-like (IF) and inorganic nanotubes (INT), are synthesized in macroscopic amounts. They were found to have superior tribological properties and can serve as solid-state additives to different lubrication fluids. More recently, metallic films incorporating the IF nanoparticles were prepared *via* wet deposition methods and also by physical vapor deposition techniques. The incorporation of the nanoparticles endows such coatings self-lubricating behavior, *i.e.* low friction and wear, which is highly desirable for variety of applications. The current feature article provides a short overview of the progress in the materials synthesis of IF and INT phases. Subsequently, a progress report of the various efforts to apply such coatings to medical devices and drug delivery is described.

1. Introduction

Over the last few decades medicine went through transformative changes where many artificial devices (intracorporeal devices) and implants are inserted to the human body for different purposes and different periods of time.[1,2] Furthermore, many of these procedures are done on ambulatory or semi-ambulatory basis, differing thereby the huge costs involved in long hospitalization of the patient and ancillary medical complications (like infections) involved in "traditional" invasive methodologies. Here, natural openings or small artificial ones pierced through the body's skin are used to insert devices in order to monitor some functionality of the human body; perform a medical procedure, or surgery. These include, among others, stents, catheters, laparoscopes, *etc.* These new treatments replace old practices where major surgical interventions under deep anaesthesia were required, leading to long healing periods and higher risk of infection. It has been predicted that, ultimately, almost every human in technologically advanced societies will host a biomaterial device in his body, at least temporarily.[3]

Notwithstanding this major progress, the fundamental difference between the surface chemistry and mechanical response of the inserted devices and the human body entail unavoidable

[a]*Department of Materials and Interfaces, Weizmann Institute, Rehovot, 76100, Israel*
[b]*Faculty of Dental Medicine, Hadassah-Hebrew University, Jerusalem, 91120, Israel*

A. R. Adini

Adi Ram Adini received her BSc (Cum Laude) in the medical sciences in 2009 (Hebrew University), and her MSc in biomedical and dental sciences (Cum Laude) in 2010. Her MSc was performed under the joint supervision of Prof. Reshef Tenne and Prof. Meir Redlich. Her Master thesis was awarded the Yael and Uri Michaeli prize for excellence. She is currently studying towards her D.M.D in the Hebrew University.

M. Redlich

Meir Redlich received his DMD in 1980 (Hebrew University). He became specialist in Orthodontics (Cum Laude) in 1994 (Hebrew University). In 2001 he earned a PhD in Oral Biology (Hebrew University). He joined the department of Orthodontics in Hadassah Medical Center-Hebrew University in 1998, where he was promoted to senior lecturer in 2004 and Associate Professor (2010). Since then he is the director of research activities in the department. He was the director of the postgraduate program in Orthodontics (2003–2006). During the last decade he gained multiple national and international research grants.

harsh interactions between the inserted devices and the different tissues. Frequently also, artificial devices are inserted through narrow body constrictions, like arteries, veins, urethra, *etc.* The outcome of such medical procedures may lead to unforeseen complications, sometimes of severe consequence. Artificial implants, such as hip replacements or artificial knees, which remain in the body for as long periods as possible (indwelling devices), suffer from a mechanical-chemical wear, often combined with obstructions and infections. In other cases, like stents and catheters, that are inserted to the urethra, encrustation of mixed biofilm-inorganic residues leads to severe morbidity for the patient and can lead to complete blockage of the fluid flow.[4] In the worst case scenario this leads to the "gluing" of the stent to the tissue requiring a more severe pull-out intervention.

Biodegradable polymers have been progressively applied to various aspects in medicine especially orthopedics.[5] These synthetic materials, particularly lactide and glycolide, offer physicians an alternative to avoid a second operation either to replace or remove the non-degradable devices such as fixation components like bone screws and suture anchors. The safety and the biocompatibility of the biodegradable polymers, as well as their full disposal from the body, has been documented in the medical literature. The implementation of the IF nanoparticle coatings is, at this stage, suitable for various medical non-degradable devices. It is assumed that following the reveal of the body removal pathways for the IF nanoparticles, the required adaptation of the IF coatings to the biodegradable polymers would be feasible, obviously subject to the healthcare benefit of such coatings.

Many of the inserted devices are made of superelastic nickel-titanium (Nitinol-NiTi) shape memory alloys which can undergo fatigue and eventually total failure (for example, NiTi endodontic files, used during root canal treatment).[6] Thus, failure of root canal files can lead to tooth loss. Biofouling, *i.e.* sedimentation of body residues and bacteria jeopardizes the functionality of many of the long term implants, like titanium-based dental implants, leading to complications due to infection hazards.

Serious attempts to counteract these unwieldy effects by different surface coatings have been documented in the literature. Active coatings which contain slowly released drugs led to major improvements in stent biofouling.[7] New coatings, including, for example, diamond-like carbon (DLC) films,[8] are making headway into daily medical practices. In this vein, new coatings and formulations containing fullerene-like nanoparticles of WS_2 and MoS_2 (hereafter named IF-WS_2 and IF-MoS_2) exhibiting excellent lubricating behavior, have been explored to address some of the above medical issues. Inorganic nanotubes (INT) of these and other compounds are studied in relation with drug delivery carriers; for biocompatible nanocomposites, *etc.*

The purpose of the present feature article is twofold, *i.e.* to summarize the progress which has been achieved so far with IF nanoparticles in the field of medical technology, and to discuss the issues and provide some prospect for future progress. It is by no means the intention of the present article to discuss comprehensively the vast literature of materials issues which are suitable for medical insertion devices. Biocompatibility issues have been discussed in numerous works[9,10] and will be only briefly mentioned in the present paper. In particular, the toxicity of the inorganic fullerene-like (IF) nanoparticles and nanotubes (INT) has not been studied in great detail until recently, when some applications of these nanomaterials, as *e.g.* solid lubricants, have emerged. Some recent progress in this respect is nonetheless reviewed, but much more work is needed if these materials are to be commercially exploited on a large scale. In a variety of applications, nanoparticles, and in particular the IF and INT powders, constitute a minority phase in solids (metal, polymer) matrices or in fluid suspensions. Therefore, the biocompatibility of the entire system must be elaborated. In particular, it is well established[9] that the most biocompatible metal alloys are based on either chromium-cobalt or titanium alloys. Electrodeposition of chromium-cobalt thin films is used in medical technology, while titanium alloys are generally deposited using vacuum techniques, like chemical and physical vapor deposition. Recently, electrodeposition of titanium alloys from ionic liquid solutions has been documented.[11]

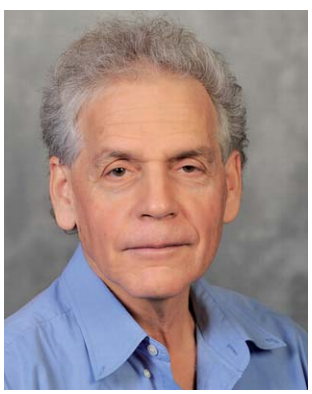

R. Tenne

Reshef Tenne earned his PhD in 1976 (Hebrew University). He joined the Weizmann Institute in 1979, where he was promoted to professor in 1995. He headed the Department of Materials and Interfaces and was the director of the Schmidt Minerva Center (2001–2007) and the Helen and Martin Kimmel Center for Nanoscale Science (2003–2011). He holds the Drake Family Chair in Nanotechnology (2004–). He received the MRS Medal (2005); The Kolthoff Prize of the Technion (2005); Israel Vacuum Society Science Prize (2005); Landau Prize in Nanotechnology (2006); MRS Fellow; the Israel Chemical Society Prize and the Advanced Research Grant (ERC) in 2008. He was elected to the Israeli Academy of Sciences and Humanities (2011) and became a Fellow of the Royal Society of Chemistry (2011). He was also recently awarded the CNR Rao Lectureship award of the Indian Chem. Research Society (2012).

2. Materials issues

2.1. Preface

Much has been published on the subject of inorganic nanoparticles with fullerene-like structures (IF) and inorganic nanotubes (INT). It was found that hollow cage structures, *i.e.* IF and INT can be obtained from inorganic compounds with layered structure. This situation is analogous to the case of carbon fullerenes and nanotubes, which are derived from a graphite lattice, *i.e.* they are based on sp^2 bonding between carbon atoms to its three nearest neighboring atoms. By folding along one direction, multiwall nanotubes are obtained, while folding along two axes leads to hollow quasi-spherical nanostructures. Probably, the mostly studied compounds forming IF and INT nanostructures are WS_2 and MoS_2. Fig. 1a,b provide scanning

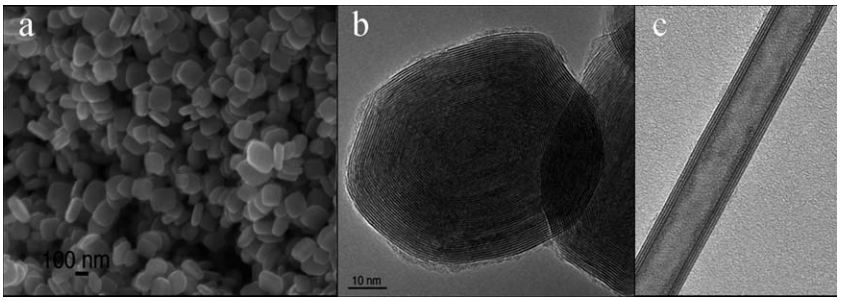

Fig. 1 Scanning (a) and transmission (b) electron microscopy (SEM and TEM, respectively) micrographs of typical IF-MoS_2 nanoparticles. Adapted from ref. 13. Fig. 1c shows 4-wall WS_2 nanotube (interwall distance is 0.62 nm).

and transmission electron micrographs of typical fullerene-like nanoparticles and nanotubes (Fig. 1c). For recent reviews on this field, the reader is referred to refs 12–14. These nanomaterials have been shown to exhibit very good mechanical and tribological properties. They are commercially used as additives to fluid lubricants; greases and also as part of self-lubricating coatings. Recent progress suggests that the applications for reinforcing polymer nanocomposites could be foreseen in the near future.

The mechanistic aspects of their synthesis have been discussed in detail. There are a number of possible ways to synthesize the IF and INT of MoS_2 and WS_2 in high yields. The use of metal oxides and H_2S as precursors was investigated in great detail and permitted scaling up of their production (see for example ref. 15–18). Some recent progress in the synthesis of such fullerene-like nanoparticles and nanotubes, is noteworthy.

2.2. Scaling up of the IF-MoS_2 synthesis

Scaling-up of the synthesis of IF-MoS_2 powder to a few g/week, using molybdenum oxide powder and H_2S gas was described in a recent work.[18] This work paved the way for a systematic study of some of the properties of these nanoparticles, including their excellent mechanical and tribological behavior.

2.3. Scaling up the INT-WS_2 synthesis

In another major recent progress, the scaling up of the synthesis of multiwall WS_2 nanotubes to kg quantities, starting from WO_3 and H_2S gas was described.[17] Fig. 2 shows a scanning electron microscopy (SEM) image of such nanotubes. Their uniformity and crystalline perfection has been vindicated through detailed analyses, using a variety of analytical tools. Not surprisingly therefore, their mechanical properties are quite remarkable.[19] Consequently, numerous studies which make use of these nanotubes are underway. A variety of future commercial applications, *e.g.* for strengthening nanocomposites, sensors for health monitoring, *etc.*, can be envisaged.

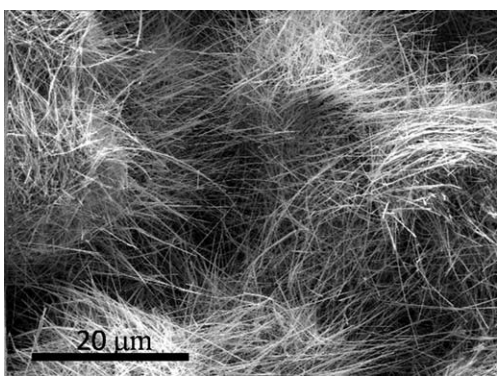

Fig. 2 SEM image of WS_2 nanotubes produced by the scaled-up process (ref. 17a).

2.4. Doping of IF and INT-MS_2 (M = Mo,W)

Another progress involves doping the IF-MoS_2 (IF-WS_2) and nanotubes thereof.[20] Here some 0.1 at% of a foreign atom, like rhenium or niobium, is added to the nanoparticles either during the synthesis or *a-posteriori*, through a high temperature diffusion process. The rhenium (niobium) atoms substitute molybdenum (tungsten) atoms in the lattice, leading thereby to the injection of an extra electron (hole) to the conduction (valence) band of the nanoparticle. This charge is trapped at or close to the surface by a process yet to be understood. The negatively (positively) charged nanoparticles can be regarded as surface charged colloids which repel each other at close proximity leading to stable suspensions. When added to oil suspensions they provide superior tribological behavior to the oil formulated with the undoped IF nanoparticles.[20]

2.5. MoS_2 nanooctahedra

Nanooctahedra of MoS_2 are considered to be the smallest hollow closed structures of that compound *i.e.* the true MoS_2 fullerenes.[21] They are synthesized by pulsed laser ablation. Fig. 3 shows a TEM image of an assortment of MoS_2 nanooctahedra obtained by pulsed laser ablation. These nanooctahedra were shown to be stable moieties in a range of 10^3–10^5 molybdenum and sulfur atoms (3–7 nm in size).[22] Furthermore, detailed theoretical calculations showed that these nanoparticles exhibit metallic character.[23] More recently, larger (up to 5×10^5 atoms) *hybrid* nanoparticles consisting of a hollow nanooctahedron in the center sheathed by a few closed MoS_2 layers with a quasi-spherical shape, were produced by a highly focused solar beam.[22] Fig. 4 shows a TEM image of a typical hybrid MoS_2 nanoparticle. Such nanoparticles are expected to exhibit a size-dependent metal to semiconductor transition. However, so far they could not be synthesized in large amounts and isolated.

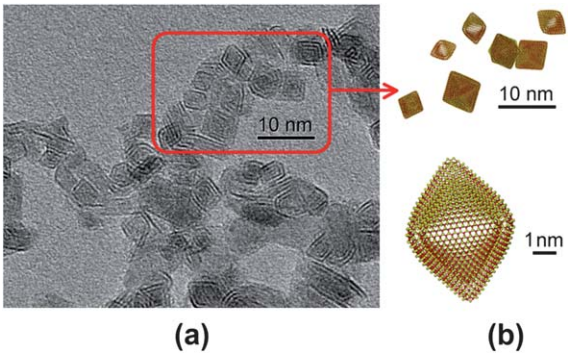

Fig. 3 (a) Transmission electron microscopy (TEM) image that includes MoS_2 nanooctahedra generated from MoS_2 powder by PLA. Note the large number of nanooctahedra with two or three layers and *ca.* 3–5 nm in size. (b) Ball-and-stick models showing assorted projections of the nanooctahedra in (a), where Mo atoms are red and S atoms are yellow. Adapted from ref. 23.

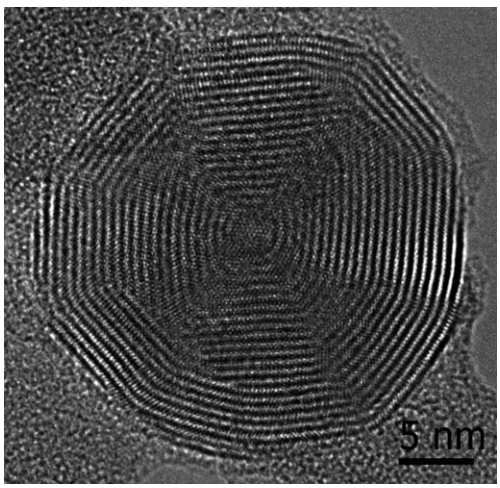

Fig. 4 Typical MoS_2 closed hybrid nanoparticles. The nanoparticle consists of a hollow nanooctahedral core (10 layers) sheathed by a shell made of 10 layers with a quasi-spherical structure. The hybrid nanocluster has a diameter of *ca.* 26 nm and consists of some 20 layers. Adapted from ref. 23.

Consequently a systematic study of their properties is still lagging behind.

2.6. Synthesis of IF and INT from volatile compounds

A great deal of progress has been realized in recent years with the synthesis of IF-MoS_2 nanoparticles and the like from volatile compounds. Here, the vapor of metal carbonyls,[24] or metal halides[25] was reacted with H_2S gas or sulfur vapor. One of the great advantages of this technique is that, by mixing metal precursors, facile synthesis of mixed IF nanoparticles, like IF-$Mo_xW_{1-x}S_2$ and others could be accomplished. Another advantage is that the reaction goes inside out, *i.e.* starting from a small nuclei and progressing outwards.[25] The nanoparticles grow very rapidly to their definite size of about 100 nm. In a recent feature article, Tremel and co-workers[26] discussed several growth mechanisms of the IF nanoparticles. In particular, the metal–organic chemical vapor deposition (MOCVD) growth of IF-MS_2 (M = Mo,W,Re) nanoparticles was described in terms of a two stages model. In the first step, the volatile metal carbonyl compound reacts with sulfur vapor, forming spherical and amorphous MS_{2+x} nanoparticles. Subsequent high temperature annealing leads to a loss of excess sulfur and crystallization from outside in. The more compact MS_2 layers arrange in closed cage structure. Upon completion of the crystallization, a hollow IF-MS_2 nanoparticle is obtained.

2.7. Functionalization of IF and INT-MS_2 surfaces

Recent progress with the functionalization of IF-MS_2 (W,Mo, Re) and INT-WS_2 nanoparticles has been reported.[27–30] Several strategies were undertaken, most of them through the work of Tremel and co-workers.[27–29] In one such strategy,[26,27] scorpionate-type ligands such as nitrilotriacetic acid (NTA) is used to immobilize functional molecules on the outer sulfur layer of the IF nanoparticle (INT). A transition-metal cation with a high sulfur affinity and octahedral coordination, like Ni^{2+}, is used to anchor the NTA to the MS_2 surface. The coordination sphere of this metal ion is blocked completely on one side with an umbrella type chelating ligand, while the other part of the coordination sphere remains open for docking to the sulfur layer of the nanotube. A polymer is attached to the NTA in order to provide binding sites for various functional groups. One such group is a fluorophore which can be excited by laser light and help identifying the location of the nanotube (IF). Other moieties provide solubility in either polar or non-polar solvents. For example, water-soluble nanotubes with a hydrophobic interior were prepared from bottlebrush copolymers with triblock copolymer branches.[31] Furthermore, biological markers can be attached to the polymer chain, which can then target pathogenic cells and serve also in drug release capacity. In another route,[29] the MS_2 fullerene-like nanoparticles and nanotubes were decorated by metal oxide nanoparticles. In the case of MnO nanoparticles the surface decoration of WS_2 nanotubes could be executed reversibly. Using an alternative chemical strategy, the IF nanoparticles were functionalized by attaching silane groups to oxide moieties at surface defects.[30] This strategy was shown to lead to improved stability and longer lifetime for IF-oil suspensions and hence to an improved long-term tribological performance for such oil suspensions.

2.8. VLS synthesis of SnS_2 nanotubes

Metallic nanoparticles, like those of gold, serve sometimes as catalysts to promote the growth of variety of inorganic nanowires, like GaAs and Si. It is also well accepted that the diameter of the growing nanowire is determined by the size of the catalyst nanoparticle. Generally, the growth process is attributed to vapor-liquid-solid (VLS) mechanism, whereby a liquid droplet of the gold catalyst at the top of the nanowire, decomposes the trimethyl gallium in the vapor phase. Due to the limited solubility of gallium in the gold droplet, it is secreted behind and reacts with the arsine rich vapor to produce a GaAs nanowire. In a similar vein, SnS_2 nanotubes were grown recently using bismuth as the growth promoter.[32] This process, if extended to

other 2-D compounds, may result in the synthesis of many new INTs.

2.9. Mama-tubes

MoS_2 nanotubes containing IF-MoS_2 nanoparticles in their core ("mama" tubes) were synthesized through a controlled sulfidization of $Mo_6S_2I_8$ nanowires.[33]

2.10. Core–shell nanotubes using INT-WS_2 template

Nanotubes were used as a template to prepare core–shell nanotubes, such as PbI_2 nanotubes inside the hollow core of the WS_2 nanotubes (PbI_2@WS_2), using different chemical routes.[34]

2.11. Thin films incorporating IF(INT)-MS_2

Enabling technology with a wide spectrum of applications was developed by deposition of coatings with IF nanoparticles incorporated into the film matrix.[35] Fig. 5 shows SEM micrograph of a cobalt film containing *ca.* 5 at% IF-WS_2 nanoparticles. The composition of the film was verified using EDS analysis. Tribological tests confirmed that the nanoparticles endow the film self-lubrication behavior with a reduced friction coefficient and wear as compared to the native metal surface.

Fig. 6 shows the results of a pin on disk test of a stainless steel coupon coated with a cobalt thin film which contains about 5 at % of IF-WS_2 nanoparticles. Obviously, the IF nanoparticles endow self-lubrication behavior to the sample. Much of the work so-far has focused on a given set of metallic coatings, like nickel, cobalt and others. Furthermore, the deposition methods were almost exclusively based on wet techniques, *i.e.* chemical bath deposition (electroless) and electrodeposition. Future work will most certainly be extended to physical vapor deposition techniques and metals such as titanium and aluminum which cannot be easily deposited by wet techniques.

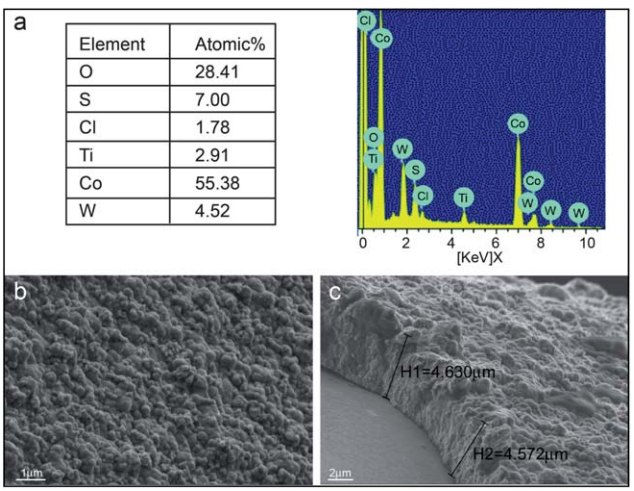

Fig. 5 (a) EDS analysis (20 keV beam) of a typical Co/IF film deposited onto various medical devices (endodontic file in this case). (b,c) SEM images of an endodontic file coated with Co/IF film. The coating was prepared, at a current density of 12 mA cm^{-2}, for a period of 6 min. The nanoparticles are clearly visible as protrusions from the cross section of the film and its surface. Adapted from ref. 48.

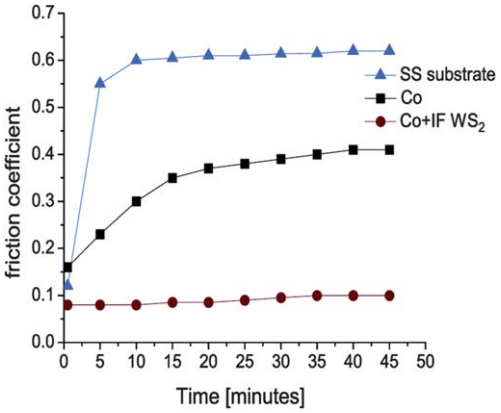

Fig. 6 Time evolution of the friction coefficient for SS coupon and different coatings electrodeposited on this substrate. Adapted from Friedman *et al.*, *Nanotechnol.* 2007, **18**, 115703.

3. Preface to medical applications of the IF nanoparticles

After reviewing in brief the recent advances in the synthesis of fullerene-like nanoparticles and nanotubes from 2-D MS_2 compounds, the time is ripe to describe the progress in the medical research front, *i.e.* potential medical applications of these nanoparticles. It should be noted however, that the research in this direction is quite new, *i.e.* some 6-years old and is limited to a very few research groups. For example the important issue of biocompatibility of the IF-MoS_2 nanoparticles has been studied very succinctly[36] so far. Preliminary data showed no apparent toxic effect of the IF-WS_2 nanoparticles.[37–39] Medical applications of these nanoparticles will require elaborate studies of their potential toxicity and biocompatibility. Such studies are currently underway and will be reported in the next few years.

One major concern in identifying a new medical application for a given device is to find a proper working model for testing the technology. This model set-up must exhibit the salient features of the real working environment for the medical device in the human body. At the same time this model must produce quantitative criteria for comparison of the new device with the existing technology. This approach delays the use of animals for the stage where the device has shown clear evidence of improving the concurrent medical technology. A few examples to that effect will be demonstrated, while others are currently under investigation.

4. Biomarkers, drug delivery and release

Nanoparticles are investigated as a platform for new medical practices, like biomarkers; vehicles for drug delivery; for hypothermia treatment; imaging contrast agents and for variety of other therapeutic practices.[40] The nanoparticles must be surface functionalized in order to render them soluble and at the same time confer adequate selectivity, specificity and reactivity; for example when used to remove a tumor. Much of the development work of IF-MS_2 nanoparticles for these kinds of therapeutic strategies has been done by Tremel and his collaborators. This work is described in a number of papers and a summary of the progress can be found in ref. 12. Here an enzyme, like silicatein, is

immobilized on the nanotube's surface. The enzyme is subsequently used to produce biotitania film onto the nanotube surface.[12] In another work, porphyrin molecules were immobilized onto the surface of IF-ReS_2 nanoparticles.[29a] The conjugated porphyrin molecules can be sensitized by near UV-visible light and fluoresce, which is a basis for a photodynamic therapeutic (PDT) treatment for several kinds of cancer. This work demonstrates the potential of the IF nanoparticles to serve as the carrier for the PDT therapeutic agent, or for optical signaling. In the same vein, terpyridine ligands were immobilized on the surface of IF-ReS_2 nanoparticles.[29b] The ligands were conjugated to different moieties which on the one hand provided solubility and on the other hand biological functionality to the nanoparticles. Polyethylene glycol (PEG) is routinely tethered to nanoparticles' surfaces and confers solubility to the nanoparticles in aqueous solutions.

5. Orthodontic wires

Recent results show that a large spectrum of potential medical applications, including coatings for orthodontic wires, catheters, stents and others, could benefit from the superior tribological behavior of the IF nanoparticles. In orthodontics abnormally positioned teeth are pushed to their correct position by application of a continuous mechanical load (orthodontic force) on the tooth, which enables their movement. Orthodontic tooth movement is controlled by rigid stainless steel (SS), or nickel-titanium (Nitinol) wires. The wires are inserted into slots of orthodontic brackets, which are bonded onto the teeth (Fig. 7a). An inevitable frictional force that resists the tooth movement interferes with this motion. To overcome this large (quasi-static) friction force, a greater orthodontic force than is actually needed to move a tooth is applied. A few studies found that 40–60% of the orthodontic force is aimed at overcoming the frictional resistance.[41] Fig. 7b shows schematics of the orthodontic treatment, which emphasizes the friction at the contact point between the wire and the bracket's corner glued onto the pulled tooth. Fig. 8 on the other hand shows the working model which has been devised to probe the efficacy of new orthodontic technologies.[42] Here the slanted wire is inserted into a bracket. A 150 g weight is hanging below simulating the force exerted by the back teeth, which serves as an anchor to help tract the front teeth. The angulation of the wire with respect to the bracket leads to a strong coupling between the edge of the bracket and the wire, *i.e.* a high friction force. The friction force is measured using an Instron set-up (model 4502) allowing a comparison between different orthodontic wire technologies.

In a series of papers, orthodontic wires were coated with thin metal films impregnated with IF nanoparticles.[35,43] The coatings were found to be stable and adhered well to the underlying wire substrate. Fig. 9 shows the friction force of several kinds of orthodontic wires angulated at 10° with respect to the bracket. A substantial reduction in the traction force of the Instron is observed for the wire coated with the Ni/IF film. These kinds of measurements were repeated for a number of different wires, like those made of stainless steel and Ni-Ti (Nitinol), with both cylindrical and rectangular cross-sections. In general, the coatings lead to a reduction in the pulling force of the Instron (friction) by 30–60%, pending on the angle between the wire and the bracket, as well as the metal used for the coating, and surface finish. The metallic coatings included either pure nickel; nickel-phosphorous and cobalt metal matrices. Measurements were carried out for both dry wires and wires wetted with water. Although the overall friction force was smaller by as much as 20% for the wetted wires, the overall difference between the coated and uncoated wires was maintained. This series of measurements are indicative of a potentially promising coating which may lead to substantial improvements in the orthodontic

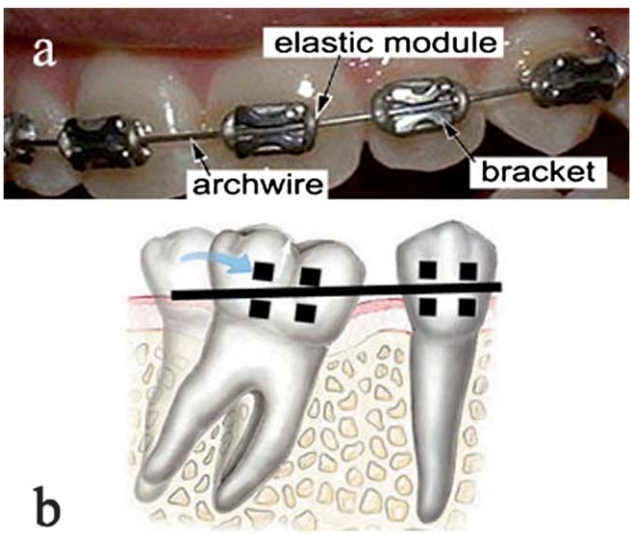

Fig. 7 (a) Picture showing the orthodontic setup with the brackets glued to the teeth and slotted orthodontic wire; (b) schematic rendering of the tilting movement of a tooth which is achieved by the orthodontic set-up. The angulation of the archwire *vis a vis* the bracket brings about a substantial increase in the friction between the two. Adapted from ref. 35.

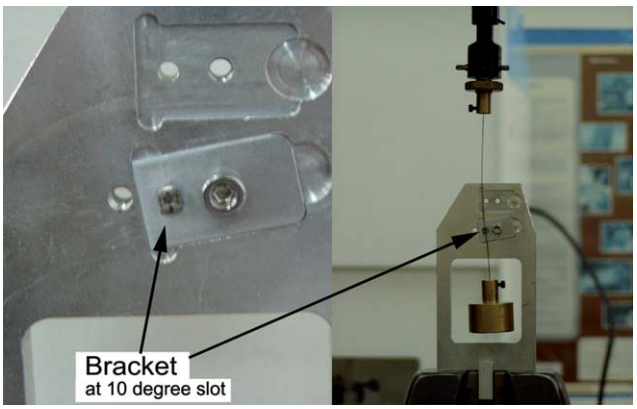

Fig. 8 A photo showing the model device used to measure the friction between the brackets and the orthodontic wire. Segments of the orthodontic wires (coated and uncoated) were attached, on their upper part, to a 10 N load cell of the Instron set-up. The lower end of the wire was connected to a 150 g weight. The wires were then inserted into the slots in the brackets and ligated with an elastomeric module (Sani-Ties Silver, GAC). The 150 gram weight was used to pull the wire similar to the clinical situation. The wires were angulated at 0–15° with respect to the bracket. Adapted from ref. 35.

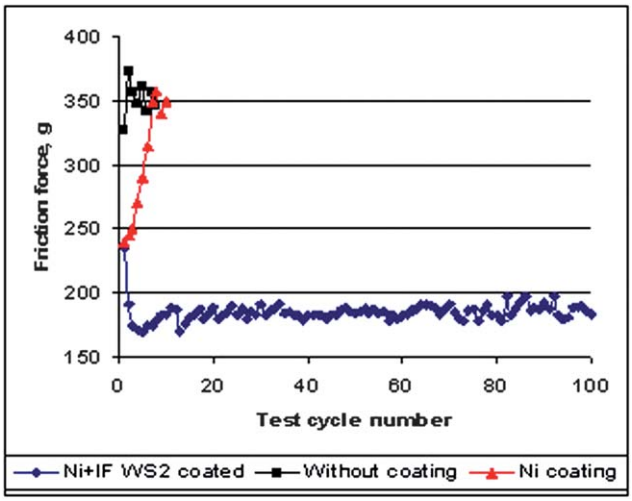

Fig. 9 Time evolution of the friction force between the bracket and the archwire (10° angulation) for various types of surface finishing of the SS orthodontic wires. Note the qualitative difference between the tribological behavior of the Ni/IF-WS_2 coated wires (in blue) and the uncoated (black curve) or Ni coated (red curve) wires. Adapted from ref. 43b.

treatment as well as shortening its duration. Future efforts should address the issue of the coatings stability under realistic conditions and its biocompatibility.

6. Endodontic files

6.1. General

NiTi (Nitinol) is a family of nearly equiatomic nickel-titanium, shape memory (SMA) and superelastic alloys with numerous applications in different walks of contemporary life. Due to its unique characteristics,[44] it is being extensively used and explored for medical applications. In the last decade, NiTi rotary instruments have become an important adjunct in endodontics, *i.e.* as files for root canal treatments (see Fig. 10).[45] NiTi files have substantially reduced the incidence of several major clinical problems in endodontics, mainly by maintaining the original shape and curvature of the canal, thus, reducing the likelihood of procedural errors. A common problem with NiTi devices, and endodontic files (EF) in particular, is their catastrophic failure (Fig. 10c).[46] In the drilling industry, it is well established that reducing the friction during the drilling process leads to improved swarf removal; overall performance and longer lifetime of the used drill.[47] In particular, diamond like carbon (DLC) coating has proved itself very useful in this respect. The same kind of thought could be applied to root canal files.

6.2. X-Ray diffraction (XRD)

Using a custom-made torsion device (Fig. 11a), the X-ray diffraction (XRD) pattern of the NiTi file was measured and

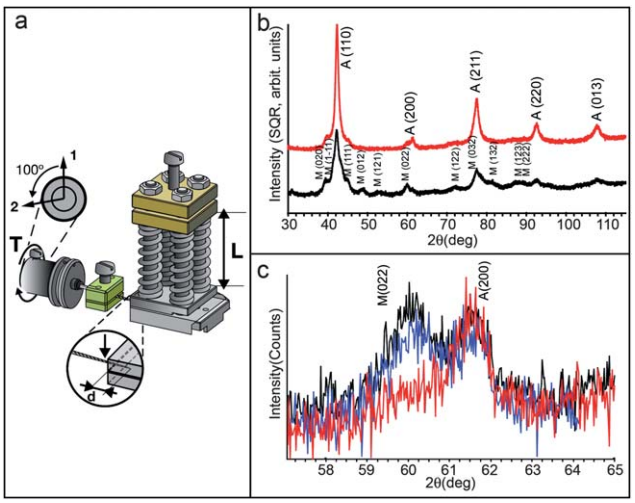

Fig. 11 XRD experiment of an EF which is being strained by a combination of clamping and twisting forces. (a) Schematic rendering of the device used for the torsion experiments of the EF. This device permits XRD examination of the file while being clamped and twisted. L- length of the spring holding the file in place. d-Insertion depth of the file between the gripping metal plates. The arrow (enlarged image) points to the place where the X-ray beam was focused. (b) The XRD pattern of the untwisted file (red curve) and the same file pattern while being twisted (black curve). (c) XRD patterns of coated (red) and uncoated (black, blue) files. The files were twisted to the same degree, and the XRD test was performed. The XRD was focused around $2\theta = 60°$ angle, where the austenite-martensite peaks are close but are distinguishable from one another. Adapted from ref. 48.

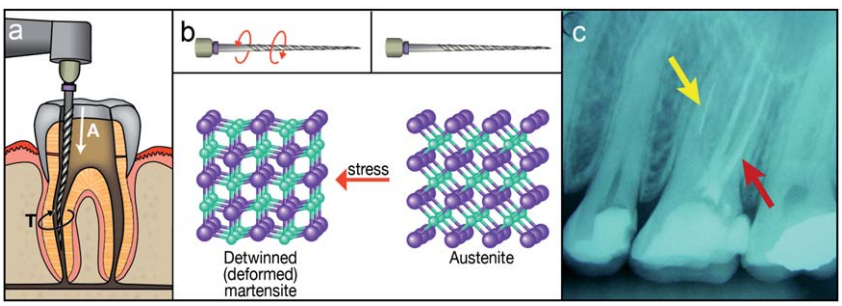

Fig. 10 (a) A schematic rendering of an endodontic file (EF) during the process of shaping and cleaning the root canal. The vector represents the torque (T) used for clockwise rotation. The vertical arrow (A) represents the direction of the apical force. (b) Structural changes of the NiTi alloy during the stress induced austenite–martensite phase transformation. When the file is twisted, the lattice transforms from austenite (cubic structure) into martensite (monoclinic). (c) Radiographic image of a tooth, following file fracture during root canal treatment. The treatment of two out of three root canals has been completed successfully (red arrow). The yellow arrow points to the broken NiTi file fractured in the third canal. Adapted from ref. 48.

subsequently analyzed while being tightly gripped by the metal supports, and twisted. The torsion device was fabricated in order to allow measuring the diffraction pattern of an EF while being subjected to combined rotational and loading stresses. This experiment bears some similarity to the real situation when the torque is exerted on the file in a constricted canal. Fig. 11b shows the XRD pattern (wide scan) of a gripped file (red curve) and of a gripped-twisted file (black curve), both uncoated. The XRD pattern of the gripped untwisted file shows that it consists mainly of an austenite phase. Twisting the file while being gripped results in a phase change for most of the NiTi crystallites in the file into (detwinned) martensite (black curve). Fig. 11c compares the XRD pattern (narrow scan) of coated and uncoated files gripped by the torsional device (Fig. 11a). First, the XRD pattern of an uncoated file was measured (black), followed by the coated file (red). The test was repeated for the uncoated file (blue) in order to ensure that no change in the apparatus occurred between the tests. The XRD analysis was focused around $2\theta = 60^\circ$ angle, where the austenite–martensite peaks are close but still distinguishable from one another.

6.3. Nanoindentation

Nanoindentation was used in order to characterize the mechanical properties of four different EFs (samples 1 to 4) which are relevant to this study. A torque rig was constructed to simulate the irreversible stress produced on a functional file (Fig. 12a). The elastic modulus (Fig. 12b) and hardness (Fig. 12c) of file tips of two pairs were compared: a fresh (pristine) file (1) and a clinically used file, discarded from an endodontic practice (2); coated (3) and uncoated (4) files subjected to the same amount of work using the torque rig (Fig. 12a) prior to the nanoindentation study. Crystallites consisting mostly of the martensite phase have been measured to exhibit Young's modulus of between 20 to 50 GPa, while austenite domains show values between 40 to 90 GPa.[49]

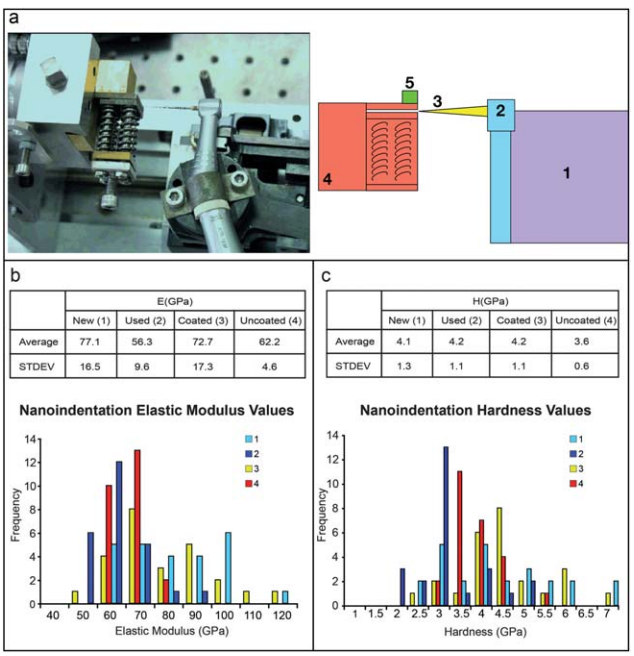

Fig. 12 (a) Image (left) and schematics (right) of the torque measuring platform (top view). 1- apical movement motor, 2- endodontic designated torque motor, 3- EF, 4- sample, 5- torque sensor. (b) Modulus (E) and (c) hardness (H) values obtained through nanoindentation experiments for: unused (new-sky blue-1) and clinically used (blue-2) files; coated file subjected to stress using the torque platform (coated-yellow-3); uncoated file (red-4) subjected to the same amount of stress as the coated one, using the torque platform. Note that the analysis indicates that the uncoated file has suffered severe fatigue. Adapted from ref. 48.

The fresh file (1-sky blue) shows a wide spread of elastic modulus and hardness values, as indicated by the relatively high standard deviations (STDV) of 16.5 GPa and 1.3 GPa respectively. It is suggested that the high spread is associated with the bimodal distribution, caused by the martensite and austenite domains, which coexist interchangeably in the sample file. The modulus and hardness results of the used file (2-blue) are much less spread out (STDV of 9.6 and 1.1 GPa), with the average elastic modulus shifted from 77.1 to 56.3 GPa. These observations could indicate a mechanical deterioration of the used file which is manifested as a low-stress related transformation. Alternatively stated, these results can be attributed to fatigue-related martensite stabilization.

In the next series of nanoindentation experiments the Co/IF coated file (3-yellow) was compared to an uncoated file (4-red). Both files went through the torque measuring test (discussed below, using the rig shown in Fig. 12a prior to the present experiment and hence are believed to have suffered some fatigue. Indeed it is seen that, both files exhibited reduced average modulus as compared with the unused file (1), as well as reduced hardness in the case of the uncoated file. Nevertheless, the reduction is moderate in the coated file (3) as compared to the uncoated one (4). In addition, the elastic modulus of the coated file exhibits a STDV which is significantly larger than that of the uncoated file (17.3 *vs.* 4.6 GPa), which may be indicative of a modest fatigue and retention of the mechanical properties of the file. Contrarily, the modulus and hardness of the uncoated file show a single peak, at much lower values (mean values of 62.2 and 3.6 GPa, respectively) which are similar to those of the clinically used file. These results suggest that the uncoated file has suffered a greater deal of fatigue during the torque tests.

6.4. Torque measurements

It was hypothesized that reducing the friction between the file with the walls of the canal (and also with the drilling swarf), will reduce the stress applied on the file and its fatigue, thereby minimizing the rate of its failures. To put this idea to the test, the initial friction of the partially gripped file (by the tension device shown in Fig. 11a) was measured using a torque measuring rig (Fig. 12a). The amount of applied torque required to achieve 100 rpm is directly related to the (dynamic) friction coefficient of the file, therefore giving an indirect estimate for this parameter. Here, a Co/IF coated file was compared to the uncoated file. The file was held by the two metal supports, which were not fully tightened in order to allow forced rotation of the file. The applied torque went down from 0.9 N cm in the case of the uncoated NiTi file to 0.27 N cm for the Co/IF coated file. These results indicate that the coating leads to a substantial reduction in the friction between the coated file and the metal support.

6.5. Torsional incidental and fatigue induced failure tests

Fig. 13 describes experiments of files rotations up to a failure, performed with the previously described platform (Fig. 12a). Two different situations were tested: In Fig. 13a the clamping force applied on the tip was relatively high, simulating the taper lock (incidental) mode of failure, where the torque exceeds the fracture strength of the file, leading to immediate failure. In this kind of test the time to failure is relatively short. Nonetheless, the test results unequivocally show that the failure of the coated file occurred after twice as long on average as compared to the uncoated file (6 s for a coated file *vs.* 3 s for an uncoated file). Moreover, the applied torque (maximal value of 0.88 N cm) on the uncoated file during this test was higher than that applied on the coated one (0.62), being consistent with the results of the friction test. These results suggest that during clinical work the coated files could exhibit lower incidental failure probability in constricted canals, where locking of the file is apparent. In Fig. 13b the clamping force holding the tip of the file was modest. The file was rotated (almost freely) back and forth—0.20 s in forward motion and then 0.10 s in a reverse direction—until fatigue-related failure occurs. This mode of failure is further evidenced by the presence of striations (shear bands due to martensite domains—see Fig. 13c and d) on the surface of the fractured area. Note that the striations appear beneath the corners of the files where load is maximum during rotation. The uncoated files failed after 6.3–7.2 min. While the coated files failed after 14–19 min.

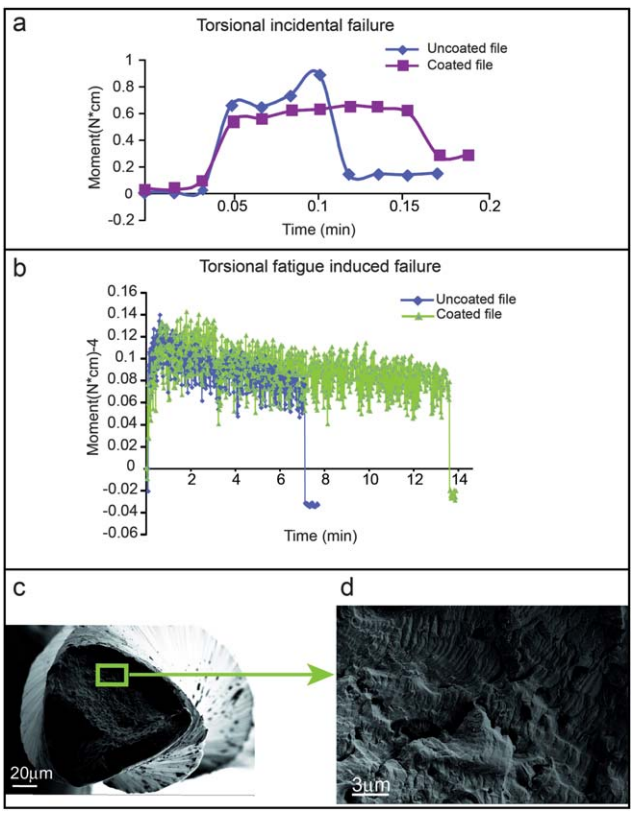

Fig. 13 (a) Incidental torsional failure test of an uncoated (blue) and coated (red) files. (b) Fatigue induced torsional failure of a coated file (green) and an uncoated (blue) file. The separation is indicated as a sudden reduction in the torque. (c,d) SEM images of the uncoated file subjected to torsional fatigue failure. On the right- enlarged image showing fatigue striation (shear bands), indicating that the breakage was related (at least in part) to fatigue. Adapted from ref. 48.

In conclusion, it was shown that IF/Co-coated EFs experience less friction, phase transformation and mechanical deterioration as compared to their uncoated counterparts. This suggests that the coated EFs might be less susceptible to breakage under work related strain, as occurs during root canal treatment. In addition, the reduced friction and subsequent torque might allow the use of NiTi EFs under conditions currently considered too risky and complicated. The proposed coating may be applicable to a wide range of NiTi-based technologies and medical applications, and is likely to have a favorable influence on the performance and lifetime of NiTi devices.

6.6. Lubricating pastes containing IF-nanoparticles

Two main lubricating agents used in endodontics were investigated: Corsodyl gel® (Chlorohexidine paste- UK, Chlorohexidine gluconate 1%) and Rc-prep® (Premier Dental, Canada, urea-peroxide 10%, ethylenediamine tetraacetic acid (EDTA) 15%). The friction coefficients were measured using a ball on flat test. Here a flat surface was lubricated by the pastes (both pristine and impregnated with IF-nanoparticles). A steel ball (AISI 1045, hardened to 45HRc) of a 2–6 mm diameter was moved at a velocity of 0.1–20 mm s^{-1}. For Rc-prep®, a friction coefficient of 0.1 ± 0.01 was measured without IF-nanoparticle impregnation, and of 0.08 ± 0.01 when impregnated with nanoparticles. With Corsodyl gel®, the measured friction coefficients were 0.33 ± 0.02 and 0.23 ± 0.02 with pristine gel and a gel mixed with IF nanoparticles, respectively (Fig. 14).[50] It is worth noting that different wt% of IF nanoparticles were mixed with the gels with the optimal concentration being reported here, *i.e.* 1 wt% for the Rc-prep® cream and 3 wt% for the Corsodyl®. Higher concentrations of IF in the Rc-prep cream resulted in degraded performance and a friction coefficient similar to those of pristine Rc-prep® cream. Rc-prep® immersed with IF-nanoparticles

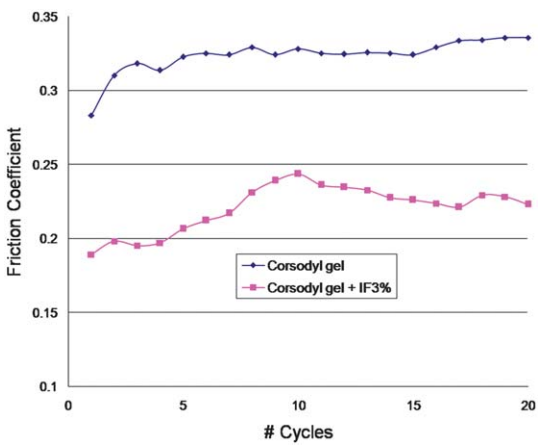

Fig. 14 Ball on flat friction coefficient (shear force/normal force) measurements of Corsodyl gel with and without IF-WS_2 nanoparticles (3 wt%). The test was performed at a load of 500 g, using a 6 mm diameter ball (pressure 1.15 GPa); velocity of 20 mm s^{-1} and stroke of 3 mm. Adapted from ref. 50.

also showed a change in color over time, suggesting that the nanoparticles react chemically with one of the ingredients in the paste. This could explain the non-linear behavior of the friction coefficient when increasing the IFs concentrations. While the reduction of friction is barely within error range for Rc-prep®, it seems that the friction coefficient of the IF formulated Corsodyl gel is substantially reduced as compared to the pristine gels. In future experiments, the modified creams will be tested in set-ups, like the one shown in Fig. 12a in order to demonstrate their efficacy under more realistic conditions.

7. Conclusions

Hollow closed (IF-WS_2) nanoparticles are currently synthesized in large amounts and are already commercially used in variety of applications, mostly for the reduction of friction and wear of mechanical systems. The synthesis of new IF nanoparticles, which exhibit more significant reduction in friction and wear, are under intensive experimentation and will be reported shortly. Advances in the synthesis of multiwall WS_2 nanotubes bring this brand of nanomaterials one step closer to the marketplace, especially in the field of high performance polymer nanocomposites.

Medicine has gone through transformative changes, whereby artificial devices are being inserted to the human body through constricted through spaces for different purposes and for different periods of time. To minimize the interaction between the human tissues and the insert, new types of coatings containing the IF nanoparticles of WS_2 and MoS_2 are being investigated. A variety of medical devices have been coated and tested so far and with new applications being currently studied. Metal electrodeposition (electroless) techniques and in the future vacuum and polymer-based coatings, with impregnated IF nanoparticles have been studied for a number of applications. These include among others: coated orthodontic wires which are inserted to brackets; endodontic files and dental creams. Furthermore, the research for using IF nanoparticles as carriers for drugs and their controlled release, or as contrast agents for imaging techniques, is in its infancy and requires much more work.

Although the efficacy of the IF nanoparticles has been unequivocally demonstrated, there is a long way for this new technology to go into practical applications. Notwithstanding the encouraging preliminary data, extensive biocompatibility tests are required for this technology. Other considerations include optimization of the deposition techniques as well as streamlining the manufacturing processes. Such efforts are currently underway in a number of laboratories.

Acknowledgements

We are grateful to Prof. Y. Moshonov and Dr B. Shay for fruitful discussions; Prof. L. Rapoport and Dr A. Moshkovich for the tribological tests; Dr R. Rosentsveig for the synthesis of the IF-WS_2 NP used in these series of experiments; Dr Y. Feldman for the XRD measurements; Dr S.R. Cohen for the nanoindentation measurements. RT gratefully acknowledges the support of ERC project *INTIF* 226639; the Israel Science Foundation; the Harold Perlman Foundation, and the Irving and Cherna Moskowitz Center for Nano and Bio-Nano Imaging. RT is the Drake Family Chair in Nanotechnology and director of the Helen and Martin Kimmel Center for Nanoscale Science.

References

1 M. Niinomi and J. Artif, *Organs*, 2008, **11**, 105–110.
2 N. B. Morgan, *Mater. Sci. Eng., A*, 2004, **378**, 16–23.
3 G. L. Shaw, S. K. Choong and C. Fry, *Urol. Res.*, 2005, **33**, 17–22.
4 J. D. Denstedt, T. A. Wollin and G. Reid, *J. Endourol.*, 1998, **12**, 493–500.
5 J. C. Middleton and A. J. Tipton, *Biomaterials*, 2000, **21**, 2335–2346.
6 (*a*) M. Balazic, J. Kopac and M. J. Jackson, *Int. J. Nano and Biomaterials*, 2007, **1**, 3–34; (*b*) P. Parashos and H. H. Messer, *J. Endod.*, 2006, **32**, 1031–1043.
7 O. C. Marroquin, F. Selzer, S. R. Mulukutla, D. O. Williams, H. A. Vlachos, R. L. Wilensky, J.-F. Tanguay, E. M. Holper, J. D. Abbott, J. S. Lee, C. Smith, W. D. Anderson, S. F. Kelsey and Kevin E. Kip, *N. Engl. J. Med.*, 2008, **358**, 342–352.
8 (*a*) G. Dearnaley and J. H. Arps, *Surf. Coat. Technol.*, 2005, **200**, 2518–2524; (*b*) N. Laube, L. Kleinen, J. Bradenahl and A. Meissner, *J. Urol.*, 2007, **177**, 1923–1927.
9 D. F. Williams, *Biomaterials*, 2008, **29**, 2941–2953.
10 S. Singh and H. S. Nalwa, *J. Nanosci. Nanotechnol.*, 2007, **7**, 3048–3070.
11 F. Endres, *ChemPhysChem*, 2002, **3**, 144–154.
12 M. N. Tahir, A. Yella, J. K. Sahoo, H. Annal-Therese, N. Zink and W. Tremel, *Phys. Status Solidi B*, 2010, **247**, 2338–2363.
13 R. Tenne and M. Redlich, *Chem. Soc. Rev.*, 2010, **39**, 1423–1434.
14 C. N. R. Rao and A. Govindaraj, *Adv. Mater.*, 2009, **21**, 4208–4233.
15 Y. Feldman, G. L. Frey, M. Homyonfer, V. Lyakhovitskaya, L. Margulis, H. Cohen, G. Hodes, J. L. Hutchison and R. Tenne, *J. Am. Chem. Soc.*, 1996, **118**, 5362–5367.
16 A. Zak, Y. Feldman, V. Alperovich, R. Rosentsveig and R. Tenne, *J. Am. Chem. Soc.*, 2000, **122**, 11108–11116.
17 (*a*) A. Zak, L. Sallacan-Ecker, A. Margolin, M. Genut and R. Tenne, *Nano*, 2009, **4**, 91–98; (*b*) A. Zak, L. Sallacan Ecker, N. Fleischer and R. Tenne, *Large-Scale Synthesis of WS_2 Multiwall Nanotubes: Update*, submitted.
18 R. Rosentsveig, A. Margolin, A. Gorodnev, R. Popovitz-Biro, Y. Feldman, L. Rapoport, G. R. Samorodnitzky-Naveh and R. Tenne, *J. Mater. Chem.*, 2009, **19**, 4368–4374.
19 I. Kaplan-Ashiri, S. R. Cohen, K. Gartsman, V. Ivanovskaya, T. Heine, G. Seifert, I. Wiesel, H. D. Wagner and R. Tenne, *Proc. Natl. Acad. Sci. U. S. A.*, 2006, **103**, 523–528.
20 L. Yadgarov, R. Rosentsveig, G. Leitus, A. Albu-Yaron, A. Moshkovith, V. Perfilyev, R. Vasic, A. L. Frenkel, A. N. Enyashin, G. Seifert, L. Rapoport and R. Tenne, submitted.
21 (*a*) P. A. Parilla, A. C. Dillon, K. M. Jones, G. Riker, D. L. Schulz, D. S. Ginley and M. J. Heben, *Nature*, 1999, **397**, 114.
22 A. N. Enyashin, S. Gemming, M. Bar-Sadan, R. Popovitz-Biro, S. Y. Hong, Y. Prior, R. Tenne and G. Seifert, *Angew. Chem.*, 2007, **119**, 631–635; *Angew. Chem., Int. Ed.*, 2007, **46**, 623.
23 A. Albu-Yaron, M. Levy, R. Tenne, R. Popovitz-Biro, M. Weidenbach, M. Bar-Sadan, L. Houben, A. N. Enyashin, G. Seifert, D. Feuermann, E. A. Katz and J. M. Gordon, *Angew. Chem., Int. Ed.*, 2011, **50**, 1810–1814.
24 J. Etzkorn, H. A. Therese, F. Rocker, N. Zink, U. Kolb and W. Tremel, *Adv. Mater.*, 2005, **17**, 2372–2375.
25 F. L. Deepak, H. Cohen, S. R. Cohen, Y. Feldman, R. Popovitz-Biro, D. Azulay, O. Millo and R. Tenne, *J. Am. Chem. Soc.*, 2007, **129**, 12549–12562.
26 M. N. Tahir, A. Yella, J. K. Sahoo, H. Annal-Therese, N. Zink and W. Tremel, *Phys. Status Solidi B*, 2010, **247**, 2338–2363.
27 M. N. Tahir, M. Eberhardt, N. Zink, H. A. Therese, U. Kolb, P. Theato and W. Tremel, *Angew. Chem., Int. Ed.*, 2006, **45**, 4809–4815.
28 M. N. Tahir, A. Yella, H. A. Therese, E. Mugnaioli, M. PanthÖfer, H. U. Khan, W. Knoll, U. Kolb and W. Tremel, *Chem. Mater.*, 2009, **21**, 5382.
29 (*a*) M. N. Tahir, A. Yella, J. K. Sahoo, F. Natalio, U. Kolb, F. Jochum, P. Theato and W. Tremel, *Isr. J. Chem.*, 2010, **50**, 500–505; (*b*) J. K. Sahoo, M. N. Tahir, A. Yella, R. Branscheid, U. Kolb and W. Tremel, *Langmuir*, 2011, **27**, 385–391.
30 C. Shahar, D. Zbaida, L. Rapoport, H. Cohen, T. Bendikov, J. Tannous, F. Dassenoy and R. Tenne, *Langmuir*, 2010, **26**, 4409–4414.

31 K. Huang and J. Rzayev, *J. Am. Chem. Soc.*, 2009, **131**, 6880–6885.
32 (*a*) A. Yella, E. Mugnaioli, M. Panthofer, H. Annal-Therese, U. Kolb and W. Tremel, *Angew. Chem., Int. Ed.*, 2009, **48**, 6426–6430; (*b*) G. Radovsky, R. Popovitz-Biro, M. Staiger, K. Gartsman, C. Thomsen, T. Lorenz, G. Seifert and R. Tenne, submitted.
33 M. Remskar, A. Mrzel, M. Virsek and A. Jesih, *Adv. Mater.*, 2007, **19**, 4276–4278.
34 R. Kreizman, S.-Y. Hong, J. Sloan, R. Popovitz-Biro, A. Albu-Yaron, G. Tobias, B. Ballesteros, B. G. Davis, M. L. H. Green and R. Tenne, *Angew. Chem., Int. Ed.*, 2008, **48**, 1230–1233.
35 A. Katz, M. Redlich, L. Rapoport, H. D. Wagner and R. Tenne, *Tribol. Lett.*, 2006, **21**, 135–139.
36 H. Wu, R. Yang, B. Song, Q. Han, J. Li, Y. Zhang, Y. Fang, R. Tenne and C. Wang, *ACS Nano*, 2011, **5**, 1276–1281.
37 G. E. Moore. *Acute inhalation toxicity study in rats–limit test. Product safety laboratories.* Study No. 18503, Dayton, NJ, USA. 2006.
38 I. Haist, *Test for sensitization (Local Lymph Node Assay–LLNA) with inorganic fullerene-like WS2 nanospheres.* Project No. 052052, BSL Disservice, Germany. 2005.
39 H. Tsabari, *Inorganic fullerene-like nanospheres (IF-WS2) Acute oral toxicity, acute toxic class method in the rat*. Final report. Batch No. HP6, Harlan Biotech, Israel. 2005.
40 (*a*) O. V. Salata, *J. Nanobiotechnol.*, 2004, **2**, 3–6, DOI: 10.1186/1477-3155-2-3; (*b*) T. Kubik, K. Bogunia-Kubik and M. Sugisaka, *Current Pharmaceutical Biotech*, 2005, **6**, 17–33.
41 A. Cash, R. Curtis, D. Garrigia-Majo and F. McDonald, *Eur. J. Orthod*, 2004, **26**, 105–111.
42 M. Redlich, Y. Mayer, D. Harari and I. Lewinstein, *Am. J. Orthod. Dentofacial. Orthop*, 2003, **124**, 69–73.
43 (*a*) M. Redlich, A. Katz, L. Rapoport, H. D. Wagner, Y. Feldman and R. Tenne, *Dent. Mater.*, 2008, **24**, 1640–1646; (*b*) M. Redlich, A. Gorodnev, Y. Feldmean, I. Kaplan-Ashiri, R. Tenne, N. Fleischer, M. Genut and N. Feuerstein, *J. Mater. Res.*, 2008, **23**, 2909–2915; (*c*) G. R. Samorodnitzky-Naveh, M. Redlich, L. Rapoport, Y. Feldman and R. Tenne, *Nanomedicine*, 2009, **4**, 943–950.
44 S. Shabalovskaya, J. Anderegg and J. Van Humbeeck, *Acta Biomater.*, 2008, **4**, 447–467.
45 O. A. Peters, *J. Endod.*, 2004, **30**, 559–567.
46 S. W. Robertson and R. O. Ritchie, *Biomaterials*, 2007, **28**, 700–709.
47 (*a*) M. Zolgharni, B. J. Jones, R. Bulpett, A. W. Anson and J. Franks, *Diamond Relat. Mater.*, 2008, **17**, 1733–1737; (*b*) V. Fox, A. Jones, N. M. Renevier and D. G. Teer, *Surf. Coat. Technol.*, 2000, **125**, 347–353.
48 A. R. Adini, Y. Feldman, S. R. Cohen, L. Rapoport, A. Moshkovith, M. Redlich, Y. Moshonov, B. Shay and R. Tenne, *J. Mater. Res.*, in press.
49 Y. O. Liu and H. Yang, *Mat Sci Eng A-Struct*, 1999, **260**, 240–245.
50 A. R. Adini, J. Moshonov, M. Redlich, Y. Feldman, L. Rapoport, A. Moshkovich, R. Tenne and B. Shay, submitted.